Direct laser writing of three-dimensional photonic crystal lattices within a PbS quantum-dot-doped polymer material

Michael James Ventura[1, 2], **Craig Bullen**[1], **and Min Gu**[1, 2]

[1]*Centre for Micro-Photonics and*
[2]*Centre for Ultrahigh-bandwidth Devices for Optical Systems*
Faculty of Engineering and Industrial Sciences,
Swinburne University of Technology, Hawthorn, Victoria 3122, Australia
mgu@swin.edu.au

Abstract: We report on the synthesis of a homogenous PbS quantum-dot-doped polymer material of thickness up to 100 micrometers. It is shown that high quality micro-void channels of submicrometer diameters can be directly fabricated into this nanocomposite by using an ultrafast femtosecond laser beam. Periodically stacked channels in the form of a three-dimensional photonic crystal woodpile lattices reveals a main stop gaps as well as higher-order gaps that overlaps the near-infrared emission wavelength range of PbS quantum dots. These partial stop gaps are well defined in an angular range from zero to 15 degrees in the stacking direction.

OCIS codes: (220.4000) Microstructure fabrication; (160.5470) Polymers; (999.999) Nanocrystal quantum dots; (999.9999) Photonic crystals.

References and links

1. H. Misawa, and S. Juodkazis, eds., *3D laser microfabrication, Principles and applications* (Wiley-Vch Verlag, Weinheim, 2006).
2. D. Day, and M. Gu, "Formation of voids in a doped polymethylmethacrylate polymer," App. Phys Lett. **80**, 2404-2406 (2002).
3. M. J. Ventura, M. Straub, and M. Gu, "Void channel microstructures in resin solids as an efficient way to infrared photonic crystals," App. Phys Lett. **82**, 1649-1651 (2003).
4. M. Straub, M. Ventura, and M. Gu, "Multiple higher-order stop gaps in infrared polymer photonic crystals," Phys. Rev. Lett. **91**, 043901 (2003).
5. E. G. Gamaly, S. Juodkazis, K. Nishimura, H. Misawa, and B. Luther-Davies, "Laser-matter interaction in the bulk of a transparent solid: Confined microexplosion and void formation," Phys. Rev. B **73**, 214101 (2006).
6. S. Juodkazis, K. Nishimura, S. Tanaka, H. Misawa, E. G. Gamaly, B. Luther-Davies, L. Hallo, P. Nicolai, and V. T. Tikhonchuk, "Laser-induced microexplosion confined in the bulk of a sapphire crystal: Evidence of multimegabar pressures," Phys. Rev. Lett. **96**, 166101 (2006).
7. E. N. Glezer, M. Milosavljevic, L. Huang, R. J. Finlay, T. H. Her, J. P. Callan, and E. Mazur, "Three-dimensional optical storage inside transparent materials," Opt. Lett. **21**, 2023-2025 (1996).
8. G. Zhou, and M. Gu, "Anisotropic properties of ultrafast laser-driven microexplosions in lithium niobate crystal," App. Phys. Lett. **87**, 1-3 (2005).
9. K. Yamasaki, S. Juodkazis, M. Watanabe, H. B. Sun, S. Matsuo, and H. Misawa, "Recording by microexplosion and two-photon reading of three-dimensional optical memory in polymethylmethacrylate films," App. Phys. Lett. **76**, 1000-1002 (2000).
10. K. Wundke, J. Auxier, A. Schülzgen, N. Peyghambarian, and N. F. Borrelli, "Room-temperature gain at 1.3 μm in PbS-doped glasses," App. Phys. Lett. **75**, 3060-3062 (1999).
11. V. Sukhovatkin, S. Musikhin, I. Gorelikov, S. Cauchi, L. Bakueva, E. Kumacheva, and E. H. Sargent, "Room-temperature amplified spontaneous emission at 1300 nm in solution-processed PbS quantum-dot films," Opt. Lett. **30**, 171-173 (2005).
12. L. Bakueva, S. Musikhin, M. A. Hines, T. W. F. Chang, M. Tzolov, G. D. Scholes, and E. H. Sargent, "Size-tunable infrared (1000-1600 nm) electroluminescence from PbS quantum-dot nanocrystals in a semiconducting polymer," App. Phys. Lett. **82**, 2895-2897 (2003).

#77756 - $15.00 USD Received 4 December 2006; revised 31 January 2007; accepted 8 February 2007

13. S. Hoogland, V. Sukhovatkin, I. Howard, S. Cauchi, L. Levina, and E. H. Sargent, "A solution-processed 1.53 µm quantum dot laser with temperature-invariant emission wavelength," Opt. Express **14**, 3273-3281 (2006).
14. S. A. McDonald, G. Konstantatos, S. G. Zhang, P. W. Cyr, E. J. D. Klem, L. Levina, and E. H. Sargent, "Solution-processed PbS quantum dot infrared photodetectors and photovoltaics," Nature Mat. **4**, 138-142 (2005).
15. L. Pang, Y. M. Shen, K. Tetz, and Y. Fainman, "PMMA quantum dots composites fabricated via use of pre-polymerization," Opt. Express **13**, 44-49 (2005).
16. M. A. Hines, and G. D. Scholes, "Colloidal PbS nanocrystals with size-tunable near-infrared emission: Observation of post-synthesis self-narrowing of the particle size distribution," Adv. Mat. **15**, 1844-1849 (2003).
17. L. Bakueva, I. Gorelikov, S. Musikhin, X. S. Zhao, E. H. Sargent, and E. Kumacheva, "PbS quantum dots with stable efficient luminescence in the near-IR spectral range," Adv. Mat. **16**, 926-929 (2004).
18. D. Day, and M. Gu, "Effects of refractive-index mismatch on three-dimensional optical data-storage density in a two-photon bleaching polymer," Appl. Opt. 37, 6299-6304 (1998).
19. J. Li, B. Jia, G. Zhou, and M. Gu, "Fabrication of three-dimensional woodpile photonic crystals in a PbSe quantum dot composite material," Opt. Express 14, 10740-10745 (2006).

1. Introduction

Direct writing of micro-structures in a thick solid medium has proven to be a powerful method for many photonic applications including optical data storage and photonic crystals [1-6]. Micro-explosions induced by an ultrafast femtosecond laser beam focused by a high numerical-aperture (NA) objective has facilitated the generation of micro-voids in glass [7], nonlinear crystals [8] and polymer materials [2, 9]. In particular, the low threshold power for generating voids in polymer materials allows for the fabrication of micro-void channels of a high degree of perfection [3]. This has provided a method for creating three-dimensional (3D) woodpile photonic crystal lattices with multiple-order stop gaps in the near-infrared wavelength region [4]. Another advantage of using polymer is the linear and nonlinear optical property of the photonic crystals can be engineered if semiconductor nanocrystals or quantum dots (QD) whose size determines their absorption and emission properties are doped in polymers.

It has been recently demonstrated that lead-salt nanocrystals such as PbS QDs, which have a large band gap in the telecommunication wavelength region and fabricated by colloidal solution, can be doped in various host materials for photonic device applications including room-temperature optical gain [10], amplified spontaneous emission [11], electroluminescence emitters [12], lasing [13] and photovoltaics [14]. Thus, it is expected that the combination of PbS QDs and polymers can result in functional polymer-based photonic devices including 3D photonic crystals. PbS doped films in the previous optical studies were typically a few hundred nanometers in thickness, making them unsuitable for the fabrication of 3D photonic crystals with dimensions of tens of micrometers. Although a few methods have been developed to form thick QD-doped polymer films, the colloidal stability of the QDs in the resin has been shown to be minimal for a system where monomer is pre-polymerized in the QD solution [15]. This method, however, has not been applied to near-infrared PbS QDs. The aim of this paper is to report on a method for preparing thick PbS-QD-doped polymer films, apply direct laser writing for generating 3D woodpile photonic crystals formed from micro-void channels, and understand the effect of the refractive index change caused by doping QDs on the bandgap performance.

2. Nanocomposite synthesis

PbS QDs were chosen in our experiments because they have a large band gap in the near-infrared wavelength range which matches the stop gaps of the 3D photonic crystals fabricated in NOA63 [3]. Further, it has been found that doping PbS QDs in the NOA63 resuts in less aggregation than PbSe QDs due to a cleaner chemical process. The route that was taken to achieve a homogeneous PbS QD-doped polymer involved the synthesis of semiconductor nanocrystals in a non-aqueous solution followed by surface chemistry modification. A wet chemical method based on Hines and Scholes routine [16] was used to synthesis PbS QDs.

#77756 - $15.00 USD Received 4 December 2006; revised 31 January 2007; accepted 8 February 2007

QDs were then dispersed in tetrachloroethylene (TCE) a solvent chosen for its low absorption at infrared wavelengths and finally evaluated using transmission electron microscopy (TEM) and infrared absorption microscopy. Varying synthetic conditions of lead and sulphur ratios allowed for particle size tuning, alternatively size tuning was achieved by varying the reaction time. Highly spherical QDs of mean size 4.5 nm (TEM insert Fig. 1) were obtained one minute after injection and showed a strong peak in absorption at 1.4 μm (Fig. 1). Extended reaction times of twenty minutes resulted in an equilibrium of the mean QD size of 3 nm.

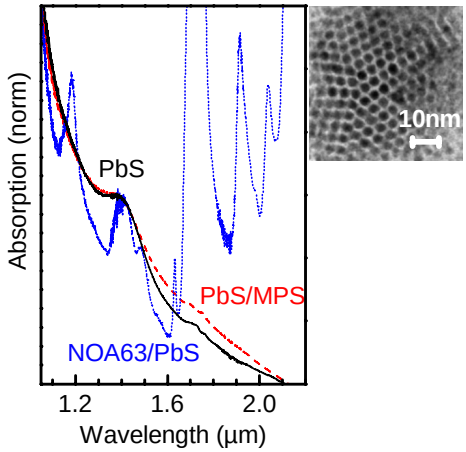

Fig. 1. Infrared transmission absorption spectra of PbS (solid black line), Mercaptopropyl-trimethoxysilane (MPS) caped PbS QDs (dashed red line) and the nanocomposite material of doped NOA63 and capped PbS QDs (dotted blue line). Insert, TEM image of 4.5 μm PbS QDs, showing their uniform shape and size.

Purified PbS QDs were doped into the commercial optical adhesive NOA63 obtained from Norland Products. This ultra-violet sensitive photo-polymerizable resin has a refractive index of 1.542 upon solidification and is transparent at infrared wavelengths. Direct doping of QDs into this material caused substantial and rapid aggregation of the QDs, and an inhomogeneous composite. Varying the dispersion solvent, QD concentration, temperature of the resin, and mixing method did little to improve the quality of the composites. To overcome this problem the surface chemistry of the QDs was altered by treatment with Mercaptopropyl-trimethoxysilane (MPS) followed by ultra-sonication [17]. In this way, homogenous nanocomposites were obtained both before and after photo-polymerization. Figure 1 illustrates that the absorption spectra pre (solid black line) and post (dashed red line) capping are unchanged suggesting that capping does not change the individual nano-crystal dimensions.

The MPS stabilized PbS QDs were then introduced by volume to the host matrix and stirred vigorously to form a homogeneous, transparent material. Samples were then sandwiching between two glass cover slips with a spacer of approximately 100 μm, which is measured by micrometer vernire caliper, and exposed to a broad UV light source for one hour. Upon solidification all the photo-initiators and TCE were removed leaving a transparent homogeneously dispersed nanocomposite. It was noted however that an upper limit existed at which aggregation of QDs prevented the synthesis of a homogeneous material. Infrared absorption microscopy of a sample doped at a low density of 0.05 parts per million (PPM) shows a peak coinciding with the QD absorption band at 1.4 μm (Fig. 1, dotted blue line) and also highlights that at low concentrations the contribution of the QD absorption in the

#77756 - $15.00 USD Received 4 December 2006; revised 31 January 2007; accepted 8 February 2007

nanocomposite is far outweighed by the inherent polymer absorptions of the matrix visible beyond 1.6 μm.

3. Characterization

To investigate that levels to which caped QDs could be loaded into the polymer host a series of samples were synthesized with increased densities of QDs, their refractive index was measured after photo-polymerization using the Becke line method [Fig. 2(a)]. The homogeneity of samples under high resolution transmission optical microscopy at 800 nm illumination with numerical aperture 1.45 was used to asses the quality of our samples (Figs. 2(b)-2(e) with a scale bar of 50 μm). At even low densities of QDs the refractive index of MPS stabilized samples was slightly higher than that of the polymerized NOA63 (0 PPM). This increase was expected as the overall refractive index of the nanocomposite is directly related to the loading levels of PbS QDs. An increase in refractive index of 0.4% was observed up to a density of 0.5 PPM of QDs. At these levels samples presented no clustering and were homogeneous [Fig. 2(c)]. For the PbS QD density beyond 0.5 PPM an increased refractive index of 1.55 was obtained for the nanocomposite, however visible aggregation of QDs into micrometer domains was observed [Figs. 2(d) and 2(e)]. Mechanical stability was still attainable up to the density of 1 PPM for aggregated materials, however beyond this point cracking and difficulties in photo-polymerizing prevented the ability to produce a solid material [Fig. 2(e)].

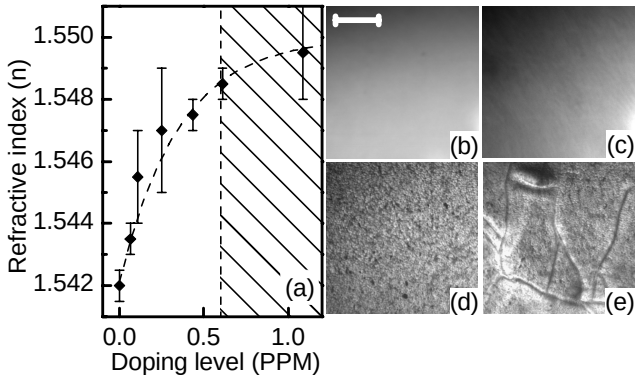

Fig. 2. (a). Refractive index as a function of doping levels (parts per million) of PbS nano-crystals to NOA63. Microscope transmission images of (b) un-doped NOA63 (50 μm scale bar), (c) nanocomposite with a PPM of 0.05, (d) nanocomposite with a PPM of 0.6 and (d) nanocomposite with a PPM greater than 1 PPM.

4. Micro-void channel woodpile photonic crystals

To explore the feasibility of fabricating complex micro devices in the homogeneous nanocomposite samples, we adopted the micro-explosion method using a femtosecond laser beam [3]. This single step, direct writing process involved the focusing of femtosecond pulsed laser light at a wavelength of 570 nm using a 100x 1.4 high NA inside the nanocomposite in the experimental setup reported elsewhere [3, 4].

3D woodpile photonic crystals were fabricated with an in-plane spacing (δx) of 1.4 μm and a layer-spacing (δz) of 1.5 μm [Fig. 3(a)]. We confirmed that up to 15 periods can be fabricated in the sample of a thickness of 100 μm which we have prepared. An example of six periods in the stacking direction (Γ-X´) with a total depth of 36 μm is shown Fig. 3. It should be noted that beyond this depth the effect of refractive index mismatch [1, 18] significantly

#77756 - $15.00 USD Received 4 December 2006; revised 31 January 2007; accepted 8 February 2007

distorts the 3D structure. Fabrication conditions were fixed to a power of 19 mW and a scanning speed 1000 µm/sec. No visible difference between individual channels was noted between the doped and un-doped materials below densities of 0.5 PPM. Infrared transmission measurements in the stacking direction showed pronounced main and higher-order photonic bandgaps in both samples at approximately 4.5 µm and 3.2 µm respectively [Fig. 3(a)]. A red shift of 125 nm is noted for the doped sample and is attributed to the increased refractive index. Iterative eigen-solving of the photonic bands in the Γ-X´ direction [4] was preformed with fixed lattice parameters as mentioned while varying the refractive index and the main and first higher-order gap positions were plotted [Fig. 3(b)]. Due to the compression of materials on formation of individual void channels the effective refractive index of the un-doped sample was calculated to be 1.67 [Fig. 3(b)], solid black line), comparable with the previously reported structures [4]. A fit with a refractive index of 1.73 was attained for the doped structure (Fig. 3(b) dotted red line), showing that indeed the nanocomposite does affect photonic bandgap positions through the increase refractive indices.

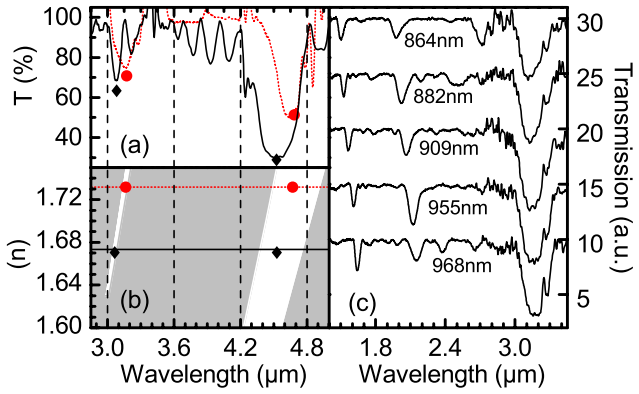

Fig. 3. (a). Infrared transmission measurements in the stacking direction of an un-doped (solid black line) and doped (dotted red line) woodpile photonic crystal lattice. A shift of the doped lattice bandgaps to longer wavelengths fits band calculations (b) where white areas denote the band positions as a function of wavelength and refractive index. (c) A series of woodpile lattices with reducing in-plane layer spacing for a fixed δz/δx of 1.1.

The performance of the nanocomposite was further characterized towards the fabrication of smaller photonic lattices which may be useful towards the field of telecommunications. Experiments were conducted in a single sample with the fabrication of woodpile lattices with a fix layer to in-plane spacing (δz/δx) of 1.1. Lattice parameters were reduced while the scanning speed was varied to produce high quality structures. Previous experiments on un-doped NOA63 showed a minimal in-plane spacing of approximately 900 nm with a layer spacing of no less than 1.3 µm, resulting in main photonic bandgaps at 3.5 µm [3, 4]. With the nanocomposite we were able to reduce the volume of the minimal unit cell by 30 %. Figure 3(c) shows the transmission spectra of a series of nanocomposite photonic crystals with reducing in-plane spacing. What can be noted form all these spectra is the presence of the main photonic bandgap above 3 µm, a first-order gap at 2 µm and a second-order gap below 1.7 µm. With the increased refractive index of the nanocomposite the strength of these higher-order gaps is increased with an average suppression of transmission for the main, first- and second-order gaps of 80, 30 and 20 % respectively.

The angular dependence of these partial stop gaps is revealed in Fig. 4, showing the transmission plot of a optimized structure over an angle range spanning from perpendicular to the stacking direction at zero degrees (Γ-X´) towards 15 degrees in the Γ-W' crystal direction.

#77756 - $15.00 USD Received 4 December 2006; revised 31 January 2007; accepted 8 February 2007

The first and second-order gaps at 1.95 μm and 1.48 μm respectively can be seen to maintain a suppression of transmission of approximately 50 % (blue bands) over an angle range of 10 degrees; beyond this angle both gaps become weaker.

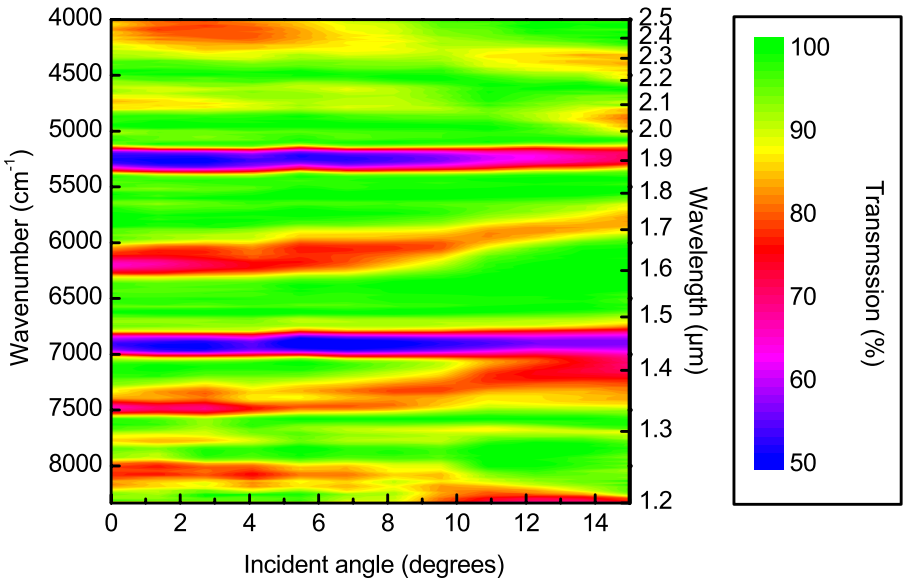

Fig. 4. Angularly resolved infrared transmission measurement of a nanocomposite woodpile photonic crystal over the angle range zero degrees (Γ-X´) towards 15 degrees in the Γ-W´ crystal direction. The lattice is transparent (green) at wavelength outside gaps. First-order and second-order gaps show a suppression of transmission of approximately 50 % (blue) over this range and are wavelength invariant.

5. Conclusion

In conclusion, we have synthesized a homogeneous thick nanocomposite material consisting of PbS QDs and a photo-polymerisable resin. Experiments have revealed that the bulk refractive index of the nanocomposite could be increased from 1.542 in the un-doped state to 1.55 after doping. High-quality photonic crystals of woodpile lattices with substantial higher-order bandgaps at telecommunication wavelengths have been realized using the micro-fabrication technique in this nanocomposite. It should be pointed out that compared with the PbSe-QD-doped resin in which two-photon polymerization is applicable [19], the surface quality of the 3D photonic crystals produced in the PbS-QD-doped 3D structures is better due to less aggregation, which is evident from the appearance of higher-order stop gaps shown Figs. 3 and 4.

Acknowledgments

This work was produced with the assistance of the Australian Research Council under the ARC Centres of Excellence Program. CUDOS (the Centre for Ultrahigh-bandwidth devices for Optical Systems) is an ARC Centre of Excellence.

#77756 - $15.00 USD Received 4 December 2006; revised 31 January 2007; accepted 8 February 2007